# Amplitude-Phase CNN-Based SAR Target Classification via Complex-Valued Sparse Image

Jiarui Deng, Hui Bi, *Member, IEEE*, Jingjing Zhang, Zehao Liu, and Lingjuan Yu

***Abstract*—It is known that a synthetic aperture radar (SAR) image obtained by matched filtering (MF)-based algorithms always suffers from serious noise, sidelobes, and clutters. However, the improvement of the image quality means the complexity of the SAR system will increase, which affects the application of the SAR image. The introduction of the sparse signal processing technique into SAR imaging proposes a new way to solve this problem. Sparse SAR image obtained by sparse recovery algorithms shows a better image performance than the typical complex SAR image with lower sidelobes and higher signal-to-noise ratio. As the most widely applied field of the SAR image, target classification relies on the SAR image with high quality. Therefore, a novel target classification model based on the amplitude and phase information of the sparse SAR image is introduced in this article. First, complex sparse image dataset is constructed by a novel iterative soft thresholding (BiIST) algorithm. Compared with typical regularization-based sparse recovery algorithms, BiIST not only can improve the quality of recovered image, but also can obtain a nonsparse solution with retaining phase information and background statistical distribution of the SAR image. Then, targets are classified by the proposed amplitude-phase convolutional neural network (AP-CNN). Typical SAR target classification networks imitate those on optical image, just using amplitude data. However, considering the particularity of the SAR image, the AP-CNN uses both amplitude and phase for training, which theoretically improves the classification accuracy. Experimental results show that the AP-CNN outperforms the typical amplitude-based CNN in target classification, both under standard operating conditions (SOCs) and extended operating conditions (EOCs). Results under SOC demonstrate that the AP-CNN improves the classification accuracy by 11.46% with only 1000 training samples. Even under EOC, the accuracy gap between the AP-CNN and CNN can reach 6.6% in the case of 800 training samples. This means that even if the number of samples is limited, the AP-CNN can obtain optimal classification result.**

***Index Terms*—Convolutional neural network (CNN), sparse synthetic aperture radar (SAR), target classification.**

## I. Introduction

SYNTHETIC aperture radar (SAR) can obtain a high-resolution image under all-weather and all-day conditions by actively transmitting and receiving electromagnetic waves, and hence, has been widely used in military reconnaissance, marine surveillance, disaster monitoring, and resource exploration fields [1], [2]. As a significant branch of SAR image processing, automatic target recognition (ATR) is a hot field in research. A typical SAR ATR system can be separated into three parts, i.e., target detection, target discrimination, and target classification [3], [4]. Target detection is mainly based on the SAR image of large scene to find the region of interest (ROI) containing targets. The most widely used detection technology is constant false alarm rate (CFAR) detector [5], [6]. The purpose of target discrimination is to eliminate false alarms caused by artificial targets in ROI, so as to facilitate subsequent target classification, that is, to classify and identify target category, model, and attribute in ROI. There are mainly three types of algorithms used for target classification, i.e., template-based methods [7]–[9], model-based methods [10], [11], and machine learning [12], [13]. As the key of template-based methods, the selection of template database determines the performance of target classification, which limits the wide application of these methods. Model-based methods overly rely on the information of target models and show high computational complexity. The key task of machine learning methods is to design a suitable set of feature extractors, which requires a lot of expertise as a foundation.

Benefiting from the growing of deep learning, a technology with automatic feature extraction has been introduced into target classification. As the first deep convolution neural network (CNN) model, AlexNet [14] achieved a 17.0% top-five error ratio in the ILSVRC [15], and thus, the CNN has become the mainstream technology for image classification. Then, in 2014, Chen *et al.* used a sparse self-encoder instead of the back propagation algorithm in the CNN to realize a multiclass classification task in SAR image, and hence, more attention is attracted into the field of radar image processing [16]. Different from optical image, SAR image contains both amplitude and phase

Manuscript received 30 April 2022; revised 4 June 2022; accepted 26 June 2022. Date of publication 29 June 2022; date of current version 7 July 2022. This work was supported in part by the National Natural Science Foundation of China under Grant 61901213, in part by Guangdong Basic and Applied Basic Research Foundation under Grant 2020B1515120060, in part by the Natural Science Foundation of Jiangsu Province under Grant BK20190397, in part by the Aeronautical Science Foundation of China under Grant 201920052001, in part by the Fundamental Research Funds for the Central Universities under Grant NE2020004, University Joint Innovation Fund Project of CALT under Grant CALT2021-11, and in part by the Science and Technology Innovation Project for Overseas Researchers in Nanjing. *(Corresponding author: Hui Bi.)*

Jiarui Deng, Hui Bi, Jingjing Zhang, and Zehao Liu are with the Key Laboratory of Radar Imaging and Microwave Photonics, Ministry of Education, Nanjing University of Aeronautics and Astronautics, Nanjing 211106, China, and also with the College of Electronic and Information Engineering, Nanjing University of Aeronautics and Astronautics, Nanjing 211106, China (e-mail: djr_919@163.com; bihui@nuaa.edu.cn; jingjingzhang@nuaa.edu.cn; liu_zh98@163.com).

Lingjuan Yu is with the School of Information Engineering, Jiangxi University of Science and Technology, Ganzhou 341000, China (e-mail: yljsmile@163.com).

Digital Object Identifier 10.1109/JSTARS.2022.3187107

information. In view of this specific property, some researchers have introduced phase of SAR image into the classification network. In 2017, Zhang *et al.* proposed the complex-valued CNN (CV-CNN) and derived the complex back propagation algorithm for the training process of the CV-CNN [17]. Compared with the CNN, the CV-CNN uses both amplitude and phase information for training. Experiments based on the polarimetric SAR image show that the CV-CNN can effectively reduce the classification error. In 2018, Coman *et al.* introduced phase information into the training process, and took the amplitude, real, and imaginary parts of SAR image as the network inputs [18]. Experimental results validate that this method can improve the classification accuracy and alleviate the overfitting problem caused by insufficient data. In 2020, Yu *et al.* proposed a new network being named as CV-FCNN for complex-valued SAR image on the basis of the CV-CNN, which replaces pooling layers and fully connected layers with convolutional layers, so as to evade complex pooling operation and avoid overfitting [19], and experiments demonstrate that the CV-FCNN shows better classification performance than the CV-CNN.

With the development of SAR image applications, the requirements for improving the performance of SAR images increase as well. How to obtain high-resolution and wide-swath images has become a significant research problem in recent years. However, when it comes to electronics, Moore's law is currently facing a bottleneck, limiting the improvement of SAR imaging systems. In addition, the Shannon–Nyquist sampling theory [20], [21] and radar resolution theory [22] are the basic laws that determine the complexity of the imaging system. In this case, high-resolution and wide-swath imaging means that the complexity of the SAR system will increase dramatically. The proposal of the sparse SAR imaging technique has provided a new solution to this problem and has gradually become the main direction of SAR imaging [23]–[26]. Compared with matched filtering (MF)-based result, a sparse SAR image shows better performance with lower sidelobes and higher signal-to-noise ratio (SNR). However, sparse SAR image recovered by regularization-based sparse reconstruction methods, e.g., orthogonal matching pursuit (OMP) [27], [28] algorithm and iterative soft thresholding (IST) algorithm [29], [30], could only improve the quality of image with ruined phase information. This will seriously restrict the further application of the sparse SAR image. In 2018, an $L_1$-norm regularization recovery algorithm named BiIST was proposed and introduced to SAR image feature enhancement [31], [32]. It is found that the BiIST can obtain two sparse estimations of interested scene, i.e., sparse solution and nonsparse solution, where the nonsparse estimation has similar background distribution to MF-based result and preserves phase information. This allows several SAR image applications, e.g., SAR interferometry (InSAR), CFAR, and the proposed classification network.

In this article, a novel classification network based on amplitude and phase information of the sparse SAR image is proposed, named as amplitude-phase CNN (AP-CNN). For the given MF-based SAR image dataset, we first improve its performance by the BiIST algorithm, so as to obtain the sparse SAR image dataset with a higher quality. Then, the amplitude and phase of the reconstructed sparse SAR image are used to form a two-channel dataset as the input of network. Finally, the SAR targets will be classified by the proposed AP-CNN based on the constructed dataset. To support our viewpoint, several experiments based on the military vehicle target samples in MSTAR [33] are carried out. Experimental results show that the AP-CNN has a better classification performance than the typical amplitude-based CNN, and has shown application potential in the case of limited samples.

The rest of this article is organized as follows. Target classification model of the proposed AP-CNN is proposed in Section II. Then, Section III describes the principle of the BiIST-based sparse SAR image recovery algorithm briefly. Experiments of the SAR target classification based on the reconstructed sparse image and results analysis are presented in Section IV. Finally, Section V concludes this article.

## II. AP-CNN-Based SAR Target Classification Framework

### A. Theory of the CNN

The CNN shows excellent feature learning ability, and has become the core technology of computer vision, which has been widely used for target classification, target identification, and image segmentation. Different from other neural networks, the local correlation and weight sharing of the CNN greatly decrease the training parameters and reduce the complexity of network. The combination of convolutional layer, pooling layer, and fully connected layer is a common structure of the CNN.

Convolutional layer contains multiple convolutional kernels, which is convolved with the feature map of the previous layer, and its result is input into the activation function to obtain the output feature map. Due to the convolution operation, output feature map and its input can be locally connected, and the local correlation in the image space enables automatic feature extraction. Weight is the important coefficient of the convolutional kernel and is updated during the training process. Weight sharing means that the value of the weight does not change in the convolution operation of the whole image. Therefore, with the reduction of parameters in the convolution kernel, both the computational overhead and the complexity of the network will be reduced. The output feature map of the convolutional layer can be expressed as

$$x_j^l = f\left(b_j^l + \sum_{i \in M^{l-1}} x_i^{l-1} * k_{ij}^l\right) \tag{1}$$

where $x_j^l$ is the $j$th feature map of the $l$th layer, and $M^{l-1}$ is the collection of feature maps of the $l$-1th layer. $k_{ij}^l$ denotes convolution kernels and $b_j^l$ is bias. $f(\cdot)$ is the nonlinear activation function whose commonly used functions are tanh, sigmoid, ReLU, LeakyReLU, etc.

According to the function of the pooling layer, it also can be regarded as a subsampling layer, usually following after the convolutional layer. Benefiting from the sampling operation of the pooling layer, the parameters and computational complexity are further reduced to prevent overfitting. Meanwhile, the output

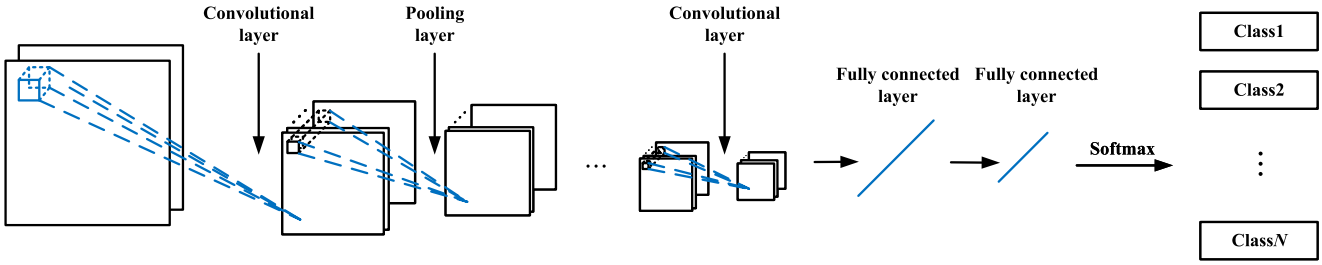


Fig. 1. Architecture of the AP-CNN.

feature map of the pooling layer exhibits a certain degree of invariance, i.e., translation invariance, rotation invariance, and scale invariance. Its output is

$$x_j^l = \text{down}\left(x_j^{l-1}, F^l\right) \tag{2}$$

where down$(\cdot)$ is the pooling function, and $F^l$ represents the size of pooling box in the $l$th layer. Pooling functions are usually set as average pooling, max pooling, min pooling, and stochastic pooling.

Unlike feature extraction in the convolutional layer and feature sampling in the pooling layer, a fully connected layer integrates features by connecting each neuron of the current layer with all neurons of the previous layer. Then, the distributed feature representations are mapped to the sample label space, so as to classify targets according to the specific task. When the CNN is used for target classification, the output layer usually adopts the softmax regression model (softmax layer), whose output prediction vectors can be written as $\boldsymbol{y} = (y_1, y_2, \ldots, y_N)^{\mathrm{T}}$ with $N$ being the number of classes.

### B. Amplitude-Phase Convolutional Neural Network (AP-CNN)

Fig. 1 shows the architecture of the proposed AP-CNN-based SAR target classification network. Similar to the CNN, convolutional layer, pooling layer, and fully connected layer form the structure of the AP-CNN, which is depicted in Fig. 2. The main characteristics of the AP-CNN are shown as follows.

1) Input layer: The input data are a two-channel SAR image dataset with amplitude layer and phase layer.
2) Convolutional layer: Batch normalization after the convolution operation can accelerate the convergence of the network and improve the stability of training process. Then, ReLU is selected as the activation function to alleviate problems of gradient vanishing and explosion.
3) Pooling layer: Average pooling operation is used in this layer to preserve the background of image.

It should be noted that different from the amplitude-based classification network, the input data of the AP-CNN is a two-channel SAR image. Taking point target as an example, the two-channel input image consists of amplitude layer [see Fig. 3(a)] and phase layer [see Fig. 3(b)]. By using this two-channel image as the input, phase information is integrated into the learning process of the training network.

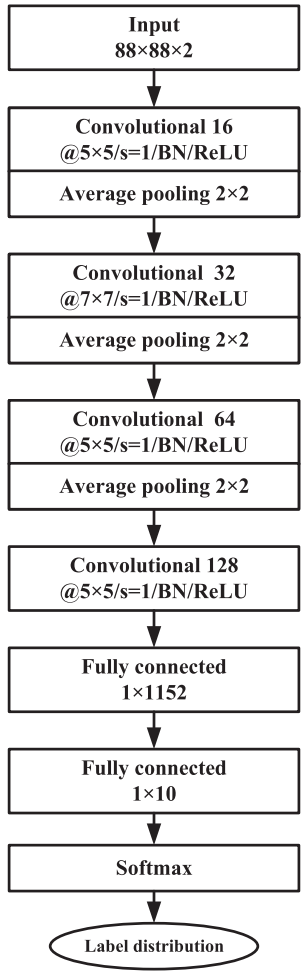


Fig. 2. Structure of the AP-CNN.

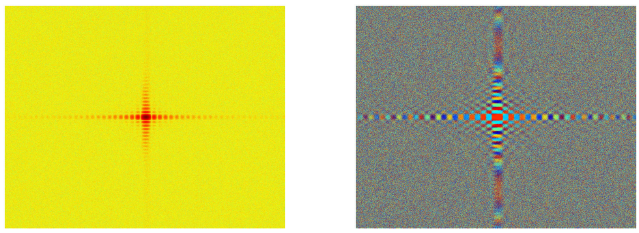

(a) (b)

Fig. 3. Input data of the AP-CNN consists of (a) amplitude layer of SAR image and (b) phase layer of SAR image.

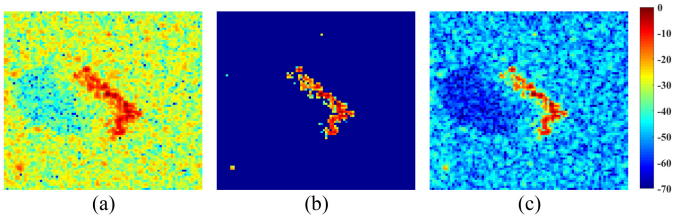


Fig. 4. SAR image recovered by different methods. (a) MF recovered image. (b) Sparse solution $\hat{\mathbf{X}}$ of BiIST. (c) Nonsparse solution $\tilde{\mathbf{X}}$ of BiIST.

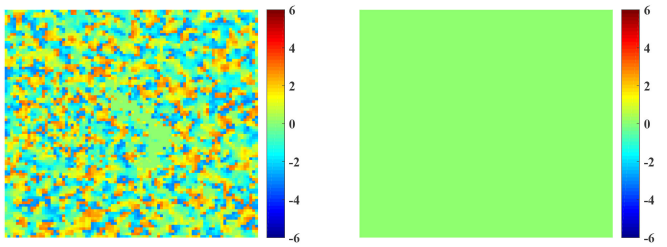


Fig. 5. Phase difference between MF-based image and (a) sparse solution $\hat{\mathbf{X}}$ and (b) nonsparse solution $\tilde{\mathbf{X}}$.

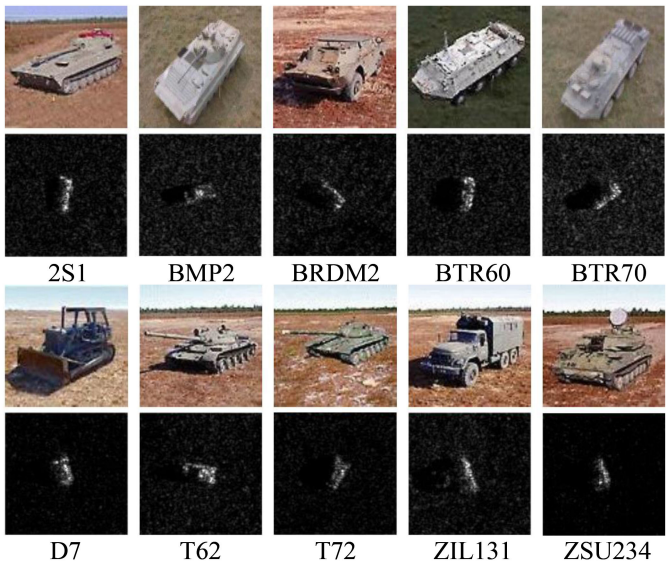


Fig. 6. SAR image and corresponding optical image of ten classes vehicles in MSTAR dataset.

TABLE I
DATA DESCRIPTION FOR SOC

| Class | Serial No. | Training set (Depression17°) | Testing set (Depression15°) |
|---|---|---|---|
| **2S1** | B01 | 299 | 274 |
| **BMP2** | SN9563 | 233 | 196 |
| **BRDM2** | E-71 | 298 | 274 |
| **BTR60** | Kloyt7532 | 256 | 195 |
| **BTR70** | C71 | 233 | 196 |
| **D7** | 92v13015 | 299 | 274 |
| **T62** | A51 | 299 | 273 |
| **T72** | SN132 | 232 | 196 |
| **ZIL131** | E12 | 299 | 274 |
| **ZSU234** | D08 | 299 | 274 |
| **Total** | | 2747 | 2426 |

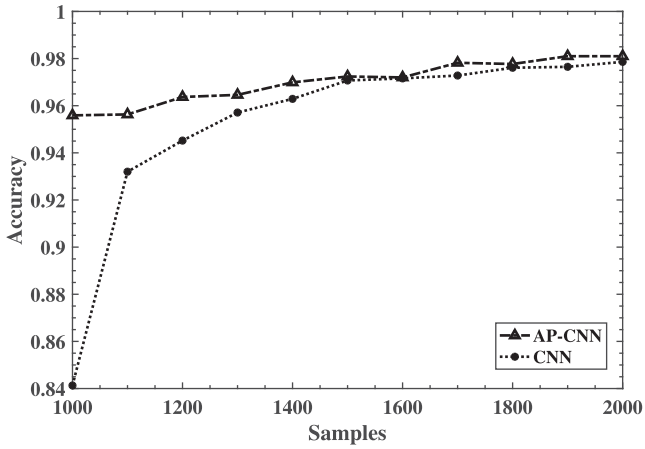


Fig. 7. Experimental results of different training samples on amplitude-based CNN and AP-CNN under SOC.

## III. BIIST-BASED SAR IMAGE ENHANCEMENT

### A. Principle

Due to data copyright and system confidentiality, MF-based SAR complex image data are usually more readily available than original echo. Therefore, in this article, a sparse SAR image enhancement algorithm based on the complex SAR image is introduced, so as to improve the quality of MF-based result. According to [31] and [32], the enhancement model is as follows:

$$\mathbf{X}_{\mathrm{MF}} = \mathbf{X} + \mathbf{N} \tag{3}$$

where $\mathbf{X} \in \mathbb{C}^{N_P(\mathrm{Azimuth}) \times N_Q(\mathrm{Range})}$ refers to the interested area, $\mathbf{X}_{\mathrm{MF}}$ is the MF recovered complex image data, and $\mathbf{N}$ stands for the difference between $\mathbf{X}_{\mathrm{MF}}$ and $\mathbf{X}$ that includes noise, sidelobes, and clutters. Then, $\mathbf{X}$ can be reconstructed by solving the $L_1$-norm regularization problem

$$\hat{\mathbf{X}} = \min_{\mathbf{X}} \left\{ \|\mathbf{X}_{\mathrm{MF}} - \mathbf{X}\|_F^2 + \beta \|\mathbf{X}\|_1 \right\} \tag{4}$$

where $\beta$ denotes the regularization parameter. As a recovery algorithm on the basis of $L_1$-norm regularization, BiIST is used in this article to deal with the optimization problem in (4) and the detailed iteration can be found in [31] and [32]. The BiIST algorithm will output two kinds of sparse images simultaneously, i.e., sparse solution ($\hat{\mathbf{X}}$) and nonsparse solution ($\tilde{\mathbf{X}}$). Similar to the sparse image recovered by traditional sparse reconstruct algorithms such as OMP and IST, sparse solution $\hat{\mathbf{X}}$ has lower noise, sidelobes, and clutters than MF-based result. However, the background distribution and phase information of $\hat{\mathbf{X}}$ are ruined. Different from $\hat{\mathbf{X}}$, the nonsparse estimation $\tilde{\mathbf{X}}$ is able to

TABLE II
CLASSIFICATION ACCURACY OF DIFFERENT TRAINING SAMPLES ON AMPLITUDE-BASED CNN AND AP-CNN UNDER SOC

| Samples | 1000 | 1100 | 1200 | 1300 | 1400 | 1500 | 1600 | 1700 | 1800 | 1900 | 2000 |
|---|---|---|---|---|---|---|---|---|---|---|---|
| **CNN** | 84.13% | 93.20% | 94.52% | 95.71% | 96.29% | 97.07% | 97.16% | 97.28% | 97.61% | 97.65% | 97.86% |
| **AP-CNN** | 95.59% | 95.63% | 96.37% | 96.46% | 96.99% | 97.24% | 97.20% | 97.82% | 97.77% | 98.10% | 98.10% |

TABLE III
CONFUSION MATRIX OF THE AP-CNN BASED ON SPARSE SAR IMAGE DATASET UNDER SOC

| Class | 2S1 | BMP2 | BRDM2 | BTR60 | BTR70 | T62 | T72 | ZSU234 | D7 | ZIL131 | Total |
|---|---|---|---|---|---|---|---|---|---|---|---|
| **2S1** | 260 | 0 | 0 | 0 | 1 | 0 | 3 | 0 | 0 | 0 | |
| **BMP2** | 3 | 191 | 2 | 2 | 2 | 0 | 0 | 0 | 0 | 0 | |
| **BRDM2** | 1 | 0 | 262 | 0 | 0 | 0 | 0 | 0 | 0 | 0 | |
| **BTR60** | 0 | 1 | 3 | 193 | 0 | 0 | 0 | 1 | 0 | 0 | |
| **BTR70** | 2 | 2 | 0 | 0 | 193 | 0 | 0 | 0 | 0 | 0 | |
| **D7** | 0 | 0 | 0 | 0 | 0 | 271 | 1 | 0 | 0 | 1 | |
| **T62** | 3 | 0 | 0 | 0 | 0 | 0 | 268 | 0 | 0 | 0 | |
| **T72** | 2 | 2 | 0 | 0 | 0 | 0 | 0 | 195 | 0 | 0 | |
| **ZIL131** | 0 | 0 | 7 | 0 | 0 | 3 | 1 | 0 | 274 | 0 | |
| **ZSU234** | 3 | 0 | 0 | 0 | 0 | 0 | 0 | 0 | 0 | 273 | |
| **Accuracy(%)** | 94.89 | 97.45 | 95.62 | 98.97 | 98.47 | 98.91 | 98.17 | 99.49 | 100.00 | 99.64 | 98.10 |

protrudes target features, and retain the background distribution of the interested scene at the same time. In addition, it also can recover the phase information of the SAR image. Therefore, it makes the phase-based SAR image applications possible, e.g., InSAR and SAR tomography (TomoSAR).

### B. Verification

Some MSTAR dataset-based experiments are utilized to validate the BiIST algorithm in the preservation of the SAR image background statistical distribution and phase information. Fig. 4 shows the MF-based result and sparse SAR image recovered by the BiIST-based algorithm, respectively. It is found that both sparse and nonsparse estimations of BiIST have a better performance than MF recovered image with a higher SNR, which will provide more effective information for the training of network. However, it should be noted that, as shown in Fig. 4(b), $\hat{\mathbf{X}}$ highlights the target with ruined background statistical characteristics, while $\tilde{\mathbf{X}}$ can retain the image statistical distribution [see Fig. 4(c)]. Furthermore, when it comes to the phase information preservation, the phase difference between the MF-based image and the results of BiIST is presented in Fig. 5. Different from Fig. 5(a), it is seen that the phase difference between the MF-based image and $\tilde{\mathbf{X}}$ equals to zero [see in Fig. 5(b)]. This means that $\tilde{\mathbf{X}}$ can achieve exact phase recovery. Due to the image quality improvement and phase preservation ability of $\tilde{\mathbf{X}}$, we will first reconstruct the sparse SAR image dataset consisting of the nonsparse solution $\tilde{\mathbf{X}}$ of BiIST for the following SAR target classification, which will theoretically improve the performance of classification based on the proposed AP-CNN network.

## IV. EXPERIMENTAL RESULTS

### A. Dataset

In this section, sparse SAR image dataset is reconstructed based on the military vehicle samples in MSTAR [33], which is a public dataset from the moving and stationary target acquisition and recognition project. Data in MSTAR are SAR image slices of ground stationary targets, including images of different classes at aspect angle ranging from $0^\circ$ to $360^\circ$. There are ten kinds of military vehicles in MSTAR and Fig. 6 shows the optical images of corresponding class. Target slices of MSTAR could be divided into standard operating conditions (SOCs) and extended operating conditions (EOCs). The BiIST algorithm is first used to obtain the sparse image $\tilde{\mathbf{X}}$ dataset based on MSTAR, and then, two-channel image is reconstructed with the first layer being amplitude and the second layer being phase. In this article, the classification results of the proposed AP-CNN and amplitude-based CNN are compared based on the reconstructed sparse SAR image dataset.

### B. Verification Under SOC

Target samples in testing set under SOC have the same serial numbers and categories as training set, and the depression angle changes by $2^\circ$. The target slices obtained with the depression angle of $17^\circ$ are used for the training set, and the depression angle of $15^\circ$ form the testing set. Table I shows the data description under SOC, containing serial number, depression angle, and the number of target samples per class in training and testing set. As shown in Table I, the dataset under SOC contains ten kinds of military vehicles. Several experiments based on multiple sets

TABLE IV
DATA DESCRIPTION FOR EOC

| Class | Serial No. | Training set (17°) | Testing set (30°) |
|---|---|---|---|
| **2S1** | B01 | 299 | 288 |
| **BRDM2** | E-71 | 298 | 287 |
| **T72** | SN132/A64 | 299 | 288 |
| **ZSU234** | D08 | 299 | 288 |
| **Total** | | 1195 | 1151 |

of training samples are carried out with samples of each class ranging from 100 to 200, so as to verify the performance of the proposed network comprehensively. Experimental results are shown in Fig. 7, and the classification accuracy of each set is listed in Table II. It is found that the AP-CNN has a better classification performance than amplitude-based CNN. When the training sample of each class is 100, the classification accuracy of the AP-CNN is 95.59% with 11.46% higher than the 84.13% of amplitude-based CNN. It also can be seen that with the decrease of training samples, the gap of classification accuracy between the AP-CNN and CNN is more obvious (see in Fig. 7). This means that the AP-CNN has a huge application potential in the case of limited samples. Confusion matrix of 2000 training samples based on the AP-CNN is presented in Table III, including target classification results and accuracy of each category.

### C. Verification Under EOC

Unlike SOC, the samples in the training and testing sets under EOC differ greatly in depression angle. The targets in training set are collected at 17° depression angle, and the depression angle of targets in testing set is 30°, 13° differing from that in the training set. Furthermore, the target types in training set and testing set are also different. Data description of each category under the EOC are listed in Table IV, including the number of targets, depression angle, and serial number. Due to the special imaging mechanism of SAR, the same type of SAR targets show great characteristic difference at different depression angles, which will bring difficulty for target classification. Table IV shows the four classes of military vehicles in the dataset under EOC. It should be noted that the type of T72 in the training set is SN132 and A64 in the testing set, which will also bring the difficulty for target classification. Similar to the experiments under SOC, the number of each class in training samples ranges from 200 to 250. Several experiments based on the reconstructed sparse SAR image dataset are carried out to compare the performance of the AP-CNN and amplitude-based CNN in SAR target classification. Fig. 8 shows the experimental results and the accuracy of each set is listed in Table V. It is shown that the classification accuracy based on the AP-CNN is much higher than that of the amplitude-based CNN, which shows a better performance in the case of increased classification difficulty. The AP-CNN can still achieve the accuracy of 90.53% when the training sample of each category is 200, with 6.6% outperforming the CNN. Table VI is the confusion matrix of 1000 training samples based on the AP-CNN, from which it can be seen that due to the different types of T72 in training and testing sets, the classification accuracy of T72 is only 85.76%, which is lower than other targets.

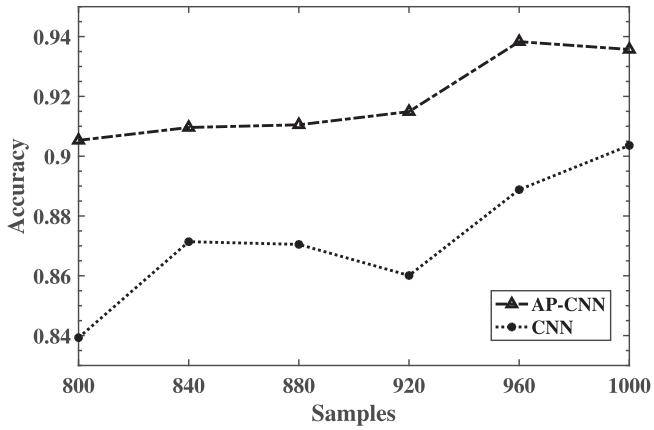


Fig. 8. Experimental results of different training samples on amplitude-based CNN and AP-CNN under EOC.

TABLE V
CLASSIFICATION ACCURACY OF DIFFERENT TRAINING SAMPLES ON AMPLITUDE-BASED CNN AND AP-CNN UNDER EOC

| Samples | CNN | AP-CNN |
|---|---|---|
| **800** | 83.93% | 90.53% |
| **840** | 87.14% | 90.96% |
| **880** | 87.05% | 91.05% |
| **920** | 86.01% | 91.49% |
| **960** | 88.88% | 93.83% |
| **1000** | 90.36% | 93.57% |

TABLE VI
CONFUSION MATRIX OF AP-CNN BASED ON SPARSE SAR IMAGE DATASET UNDER EOC

| Class | 2S1 | BRDM2 | T72 | ZSU234 | |
|---|---|---|---|---|---|
| **2S1** | 282 | 1 | 9 | 25 | |
| **BRDM2** | 6 | 285 | 18 | 0 | |
| **T72** | 0 | 0 | 247 | 0 | |
| **ZSU234** | 0 | 1 | 14 | 263 | |
| **Accuracy(%)** | 97.92 | 99.30 | 85.76 | 91.32 | 93.57 |

In this section, several experiments based on the constructed sparse SAR image dataset are carried out to validate the classification performance of the proposed network. Experimental results show that no matter under SOC or EOC, the AP-CNN shows better performance than the traditional amplitude-based CNN, indicating a great potential for application in limited samples.

## V. CONCLUSION

In this article, a novel classification network based on amplitude and phase information of sparse SAR image is proposed, named as AP-CNN. For the given MF-based SAR image dataset,

we first improve its performance by the BiIST algorithm, so as to obtain the sparse SAR image dataset with higher quality. Then, the amplitude and phase of the reconstructed sparse image are used to form a two-channel dataset as the input of the network. Finally, the proposed AP-CNN is used to classify the targets based on the novel dataset. Experiments demonstrate that the AP-CNN has a better classification performance than the amplitude-based CNN under SOC and EOC. Furthermore, it should be noted that in the case of limited training samples, i.e., 1000 under SOC, and 800 under EOC, the AP-CNN still outperforms the CNN by 11.46% and 6.6%, respectively.

## REFERENCES


[1] J. C. Curlander and R. N. Mcdonough, *Synthetic Aperture Radar: Systems and Signal Processing*. New York, NY, USA: Wiley, 1991.

[2] F. M. Henderson and A. J. Lewis, *Principle and Application of Imaging Radar*. New York, NY, USA: Wiley, 1998.

[3] D. E. Dugeon and R. T. Lacoss, "An overview of automatic target recognition," *Lincoln Lab. J.*, vol. 6, no. 1, pp. 3–10, 1993.

[4] D. E. Kreithen, S. D. Halversen, and G. J. Owirka, "Discriminating targets from clutter," *Lincoln Lab. J.*, vol. 6, no. 1, pp. 25–51, 1993.

[5] G. Gao, "A Parzen-window-kernel-based CFAR algorithm for ship detection in SAR images," *IEEE Geosci. Remote Sens. Lett.*, vol. 8, no. 3, pp. 557–561, May 2011.

[6] W. An, C. Xie, and X. Yuan, "An improved iterative censoring scheme for CFAR ship detection with SAR imagery," *IEEE Trans. Geosci. Remote Sens.*, vol. 52, no. 8, pp. 4585–4595, Aug. 2014.

[7] A. Eryildirim and A. E. Cetin, "Man-made object classification in SAR images using 2-D cepstrum," in *Proc. IEEE Radar Conf.*, Pasadena, CA, 2009, pp. 1–4.

[8] L. M. Novak, G. R. Benitz, G. J. Owirka, and L. A. Bessette, "ATR performance using enhanced resolution SAR," *Proc. SPIE*, vol. 2757, pp. 332–337, 1996.

[9] J. Zhu, X. Qiu, Z. Pan, Y. Zhang, and B. Lei, "Projection shape template-based ship target recognition in TerraSAR-X images," *IEEE Trans. Geosci. Remote Sens.*, vol. 14, no. 2, pp. 222–226, Feb. 2017.

[10] G. Magna, S. V. Jayaraman, P. Casti, A. Mencattini, C. D. Natale, and E. Martinelli, "Adaptive classification model based on artificial immune system for breast cancer detection," in *Proc. IEEE AISEM Annu. Conf.*, Trento, Italy, 2015, pp. 1–4.

[11] J. J. Gertler, "Survey of model-based failure detection and isolation in complex plants," *IEEE Control Syst. Mag.*, vol. 8, no. 6, pp. 3–11, Dec. 1988.

[12] Q. Zhao and J. C. Principe, "Support vector machines for SAR automatic target recognition," *IEEE Trans. Aerosp. Electron. Syst.*, vol. 37, no. 2, pp. 643–654, Apr. 2001.

[13] Y. J. Sun, Z. P. Liu, S. Todorovic, and J. Li, "Adaptive boosting for SAR automatic target recognition," *IEEE Trans. Aerosp. Electron. Syst.*, vol. 43, no. 1, pp. 112–125, Jan. 2007.

[14] A. Krizhevsky, I. Sutskever, and G. E. Hinton, "Imagenet classification with deep convolutional neural networks," in *Proc. Adv. Neural Inf. Process. Syst.*, Trento, Italy, Dec. 2012, pp. 1097–1105.

[15] O. Russakovsky *et al.*, "Imagenet large scale visual recognition challenge," *Int. J. Comput. Vis..*, vol. 115, no. 3, pp. 211–252, 2015.

[16] S. Chen and H. Wang, "SAR target recognition based on deep learning," in *Proc. Int. Cof. Data Sci. Adv. Analytics (DSAA)*, Shanghai, China, Oct./Nov. 2014, pp. 1–7.

[17] Z. Zhang, H. Wang, F. Xu, and Y. Jin, "Complex-valued convolutional neural network and its application in polarimetric SAR image classification," *IEEE Trans. Geosci. Remote Sens.*, vol. 55, no. 12, pp. 7177–7188, Dec. 2017.

[18] C. Coman and R. Thaens, "A deep learning SAR target classification experiment on MSTAR dataset," in *Proc. 19th Int. Radar Symp.*, Bonn, Germany, Jun. 2018, pp. 1–6.

[19] L. Yu, Y. Hu, X. Xie, Y. Lin, and W. Hong, "Complex-valued full convolutional neural network for SAR target classification," *IEEE Geosci. Remote Sens. Lett.*, vol. 17, no. 10, pp. 1752–1756, Oct. 2020.

[20] H. Nyquist, "Certain topics in telegraph transmission theory," *Trans. Amer. Inst. Electr. Eng.*, vol. 47, no. 2, pp. 617–644, 1928.

[21] C. E. Shannon, "Communication in the presence of noise," *Proc. IEEE*, vol. 72, no. 9, pp. 1192–1201, Sep. 1984.

[22] C. E. Cook and M. Bernfeld, *Radar Signals-An Introduction to Theory and Application*. Norwood, MA, USA: Artech House, 1993.

[23] B. Zhang, W. Hong, and Y. Wu, "Sparse microwave imaging: Principles and applications," *Sci. China Inf. Sci.*, vol. 55, no. 8, pp. 1722–1754, 2012.

[24] H. Bi, J. Wang, and G. Bi, "Wavenumber domain algorithm-based FMCW SAR sparse imaging," *IEEE Trans. Geosci. Remote Sens.*, vol. 57, no. 10, pp. 7466–7475, Oct. 2019.

[25] H. Bi, G. Bi, B. Zhang, W. Hong, and Y. Wu, "From theory to application: Real-time sparse SAR imaging," *IEEE Trans. Geosci. Remote Sens.*, vol. 58, no. 4, pp. 2928–2936, Apr. 2020.

[26] H. Bi, J. Deng, T. Yang, J. Wang, and L. Wang, "CNN-based target detection and classification when sparse SAR image dataset is available," *IEEE J. Sel. Top. Appl. Earth Obs. Remote Sens.*, vol. 14, pp. 6815–6826, 2021.

[27] Y. C. Pati, R. Rezaiifar, and P. S. Krishnaprasad, "Orthogonal matching pursuit: Recursive function approximation with applications to wavelet decomposition," in *Proc. 27th Asilomar Conf. Signal Syst. Comput.*, Pacific Grove, CA, USA, Nov. 1993, pp. 40–44.

[28] D. L. Donoho, Y. Tsaig, I. Drori, and J-L. Starck, "Sparse solution of underdetermined systems of linear equations by stagewise orthogonal matching pursuit," *IEEE Trans. Inf. Theory*, vol. 58, no. 2, pp. 1094–1121, Feb. 2012.

[29] I. Daubechies, M. Defriese, and C. De Mol, "An iterative thresholding algorithm for linear inverse problems with a sparsity constraint," *Commun. Pure Appl. Math.*, vol. LVII, pp. 1413–1457, 2004.

[30] H. Bi and G. Bi, "Performance analysis of iterative soft thresholding algorithm for $L_1$ regularization based sparse SAR imaging," in *Proc. IEEE Radar Conf.*, Boston, MA, USA, 2019, pp. 1–6.

[31] H. Bi, G. Bi, B. Zhang, and W. Hong, "A novel iterative thresholding algorithm for complex image based sparse SAR imaging," in *Proc. 12th Eur. Conf. Synthetic Aperture Radar*, Aachen, Germany, 2018, pp. 1–5.

[32] H. Bi and G. Bi, "A novel iterative soft thresholding algorithm for $L_1$ regularization based SAR image enhancement," *Sci. China Inf. Sci.*, vol. 62, no. 4, pp. 049303-1–049303-3, 2019.

[33] J. Diemunsch and J. Wissinger, "Moving and stationary target acquisition and recognition (MSTAR) model-based automatic target recognition: Search technology for a robust ATR," *Proc. SPIE*, vol. 3370, pp. 481–492, 1998.


**Jiarui Deng** was born in Jiangsu, China, in 1997. She received the bachelor's degree in electronic science and technology from the College of Electronic and Information Engineering, Nanjing University of Aeronautics and Astronautics (NUAA), Nanjing, China, in 2020, where she is currently working toward the master's degree.

Her research interests include sparse synthetic aperture radar image processing and application.

**Hui Bi** (Member, IEEE) was born in Shandong, China, in 1991. He received the bachelor's degree in electronics and information engineering from YanTai University, Yantai, China, in 2012, and the Ph.D. degree in signal and information processing from the University of Chinese Academy of Sciences, Beijing, China, in 2017.

From 2012 to 2017, he worked in the science and technology with Microwave Imaging Laboratory, Institute of Electronics, Chinese Academy of Sciences, China. He was a Research Fellow with the School of Electrical and Electronic Engineering, Nanyang Technological University, Singapore, from 2017 to 2018. Since 2018, he has been working with the College of Electronic and Information Engineering, Nanjing University of Aeronautics and Astronautics, Nanjing, China, where he is currently a Professor. His main research interests include sparse microwave imaging with compressive sensing, synthetic aperture radar data processing and application, sparse signal processing, and tomographic synthetic aperture radar imaging.

**Jingjing Zhang** was born in Anhui, China, in 1986. He received the B.E. degree in electronic information engineering from the University of Science and Technology of China, Anhui, in 2009, and the Doctor of Engineering degree in signal and information processing from the University of Chinese Academy of Sciences, Beijing, China, in 2017.

From 2017 to 2021, he worked with the School of Information Science and Technology, Fudan University, Shanghai, China. Since 2021, he has been with the College of Electronics and Information Engineering, Nanjing University of Aeronautics and Astronautics, Nanjing, China, as an Associate Professor. His research interests include the design, modeling and calibration of polarimetric SAR systems; SAR imaging; and polarimetric and polarimetric interferometric synthetic aperture radar signal processing and applications.

**Zehao Liu** was born in Nanjing, China, in 1998. He received the bachelor's degree in communication engineering from the College of Communication Engineering, Nanjing Institute of Technology, Nanjing, China, in 2020. He is currently working toward the master's degree with the Nanjing University of Aeronautics and Astronautics, Nanjing.

His current research interests include deep learning, transfer learning, and synthetic aperture radar image processing.

**Lingjuan Yu** received the M.S. degree in signal and information processing from the South China University of Technology, Guangzhou, China, in 2009, and the Ph.D. degree in electromagnetic field and microwave technology from the National Space Science Center, Chinese Academy of Sciences, Beijing, China, in 2012.

From 2015 to 2019, she was a Postdoctoral Fellow with the Aerospace Information Research Institute, Chinese Academy of Sciences. From 2020 to 2021, she was a Visiting Fellow with the School of Information Science and Technology, Fudan University, Shanghai, China. She is currently an Associate Professor with the School of Information Engineering, Jiangxi University of Science and Technology, Ganzhou, China. Her research interests include synthetic aperture radar data processing and application.